Magnetic, specific heat and transport properties of $U_{1-x}Th_xPt$ alloys

2000 J. Phys.: Condens. Matter 12 9897

(http://iopscience.iop.org/0953-8984/12/48/307)

J. Phys.: Condens. Matter **12** (2000) 9897–9916. Printed in the UK PII: S0953-8984(00)17224-8

Magnetic, specific heat and transport properties of $U_{1-x}Th_xPt$ alloys

V H Tran†, A Czopnik†, P de V Du Plessis‡, A M Strydom‡, R Troć† and V Zaremba§

† W Trzebiatowski Institute for Low Temperature and Structure Research, Polish Academy of Sciences, PO Box 1410, 50-950 Wrocław, Poland
‡ f-Electron Magnetism and Heavy-Fermion Physics Research Programme, Department of Physics, University of the Witwatersrand, Private Bag 3, PO Wits 2050, Johannesburg, South Africa
§ Department of Inorganic Chemistry, I Franko L'viv State University, Kirila and Mefodiya Street 6, 290005 L'viv, Ukraine

E-mail: vhtran@int.pan.wroc.pl

Received 21 August 2000

Abstract. Previous studies on UPt samples indicated ferromagnetic ordering either at $T_C = 27$ K or at $T_C = 19$ K while in some samples there was evidence of the presence of both these transitions. These differences are thought to be associated with the presence of material of different crystal structure, *viz.* a monoclinic structure for the higher-T_C material (H phase) and an orthorhombic structure for the lower-T_C material (L phase). We have studied the crystal structure, magnetization, specific heat and transport properties of the solid solutions $U_{1-x}Th_xPt$, including a pure UPt sample. We observed that the substitution of Th for U in UPt stabilizes the L phase for all compositions. Ferromagnetism is observed for $0 \leqslant x \leqslant 0.4$ and there are indications of the presence of short-range magnetic order for $x \geqslant 0.5$, which vanishes slowly up to $x \approx 1$. At low temperatures in the magnetically ordered region the magnetic and electronic contributions to the specific heat C_{5f} and electrical resistivity ρ_{5f} are described by expressions that contain the magnon energy-gap Δ. These also include the $\gamma_{5f}(0)T$ and AT^2 terms to describe the C_{5f} and ρ_{5f} temperature dependences respectively. For L-phase UPt, the low-temperature fitting (below 10 K) yields $\Delta = 19(1)$ K and $\gamma_{5f}(0) = 0.122(2)$ J K^{-2}/mol U, while the higher-temperature one (above 10 K) yields $\Delta = 35(2)$ K and $\gamma_{5f}(\mathrm{hT}) = 0.151(3)$ J K^{-2}/mol U. With Th substitution Δ decreases, but the $\gamma_{5f}(0)$ value for both the magnetically ordered and non-ordered samples remains practically unchanged, being close to that of the higher-temperature value found for this compound. The magnetoresistance is negative and large in the ordered region and becomes slightly positive at low temperatures for the Th-rich alloys. The presence of the Kondo interaction is indicated in these alloys almost up to $x \approx 1$.

1. Introduction

The ferromagnetic behaviour of UPt has been the subject of several studies on polycrystalline samples through measurements of magnetization [1–7], specific heat [2–6, 8], electrical resistivity [5, 6, 9–11], magnetoresistance, Hall effect [12], ac-susceptibility [13], thermal expansion [4] and by neutron diffraction investigations [5, 14–16]. The latter studies [14, 16] confirm ferromagnetic order at low temperatures with moments aligned along the *b*-axis of the orthorhombic unit cell of UPt. Ordered moment values at 4 K of 1.04 μ_B/U [14] and 1.1 μ_B/U [16] have been reported. The results from all these studies are puzzling, often

0953-8984/00/489897+20$30.00

conflicting and indicate a strong influence of sample preparation conditions on the magnetic properties. Most notably the coexistence of two phase transitions has been reported for some samples, one associated with the onset of ferromagnetic order at $T_C \approx 27$ K and another one seen as an anomaly in the magnetization or susceptibility near 19 K [1, 2, 5, 6, 8, 13]. Other samples showed anomalies in their physical properties only at one transition temperature, i.e. either at 19 K for samples of [3] and [4] and sample 14B of [5], or at 27 K for samples of [9], [15] and [17]. Huber *et al* [1] showed that the saturation moment of a UPt sample, with $T_C = 30$ K was reduced to 10% of this value by applying a pressure of 20 kbar. However, almost no change of T_C was observed in applying pressure. Frings and Franse [5] reported that for a sample with strong signatures of both transitions in its magnetization, a large decrease of 27% occurred in its saturation magnetization upon application of 4.5 kbar. Upon a subsequent return to ambient pressure the magnetization curve exhibited only the 27 K transition. On the other hand, their sample, which is characteristic of only the 19 K transition, showed just a few per cent change in magnetization under the applied 4.5 kbar pressure. Furthermore, in a sample showing both transitions, the transition at 19 K did not reappear after releasing pressure at low temperatures, but it is restored at room temperature [5, 13].

The two magnetic transitions of different characteristics are thought to be associated with different types of crystal structure that the compound exists in. The original assignment [18] of its structure as of the orthorhombic CrB type (space group *Cmcm*) had been accepted for many years until Dommann and Hulliger [19] proposed the monoclinic PdBi type of structure for UPt (space group $P2_1$). Neutron scattering studies [16] at ambient pressure and at 4.5 kbar suggest that the phase (henceforth designated with H) with transition temperature $T_C = 27$ K is associated with sample material of the PdBi-type structure while the 19 K transition into the L phase is associated with sample material of the orthorhombic CrB type. It is clearly preferable to study single-phase UPt samples. The structural details for our specimens will be discussed in section 2.

The only study on single crystal UPt ($T_C = 28.6$ K) that we are aware of is a very recent magnetization study of small single crystals grown by prolonged arc-melting of starting material containing an excess of In which was then evaporated [17]. The results indicate a large anisotropy between magnetization values at 5 K and 5.5 T measured along the *b*-axis (0.9 μ_B/U) compared with the *a*–*c*-plane (0.25 μ_B/U) [17], in a sample which contained the H phase only. The effective moments derived from the high-temperature approximation to the Curie–Weiss law appeared to be around 3.55 μ_B for both directions parallel and perpendicular to the *b*-axis.

In U and Ce compounds the substitution of either the f-electron element or other elements comprising the compound are often used in order to change the hybridization of f and conduction electrons and hence the strength ratio of the Rudermann–Kittel–Kasuya–Yosida and Kondo interactions. Gómez Sal *et al* [20] studied the magnetization and electrical resistivity of the UNi_xPt_{1-x} system and observed that the positive chemical pressure introduced by the smaller Ni atoms has similar effects to those observed earlier in ordinary pressure studies [1, 5]. It is noteworthy that de Podesta *et al* [8], who studied heat capacity on annealed samples of UNi_xPt_{1-x} ($0 \leqslant x \leqslant 1$), found single-phase samples practically only for $UNi_{0.8}Pt_{0.2}$ (not magnetically ordered). Their other samples were reported as being of mixed phases. The effects of dilution of U with non-magnetic La on the magnetic and transport properties of UPt have been studied by Rodríguez Fernández *et al* [11]. Magnetization curves for the $U_{1-x}La_xPt$ series show a ferromagnetic behaviour for $x < 0.5$ and paramagnetic for higher La concentrations.

In this paper we present our results of studies of the temperature and magnetic field dependences of the magnetization and electrical transport as well as the temperature dependence of the specific heat on the $U_{1-x}Th_xPt$ system.

2. Sample characteristics and experimental methods

The $U_{1-x}Th_xPt$ samples ($x = 0$, 0.1, 0.2, 0.4, 0.5, 0.6, 0.7, 0.8 and 1.0) were prepared by arc-melting the constituent elements on a water-cooled copper hearth. The samples were wrapped in tantalum foil and subsequently annealed in an evacuated silica ampoule. Both melting and annealing were carried out in an inert argon atmosphere. The Th-containing samples were annealed at 900 °C for 7 days. For UPt we report measurements on samples annealed at 650 °C for 14 days, since it turned out that for annealing at higher temperatures the UPt sample displayed characteristics of both the L and H phases described in the introduction. X-ray diffraction showed no evidence of parasitic phases or unreacted elements within the experimental accuracy. The room-temperature crystal structure of samples with $x \geqslant 0.1$ was readily determined as the orthorhombic CrB type using Cu Kα x-ray radiation. For UPt the assignment of the crystal structure proved to be more difficult because of the overlap of some of the diffraction peaks. However, use of longer wavelength x-rays from an iron tube indicated that our UPt is highly probable to be also of the CrB type, but some doubts remain. We think that the final crystal structure of this L phase can be resolved only by single-crystal refinement, that now is not available.

We thus report on the properties of UPt (L phase), which we have established to be orthorhombic within the above uncertainty, in contrast with the most recent works on UPt by Prokeš *et al* [6, 17] who report on samples which were predominantly of monoclinic structure (H phase). We have found in our investigation of the $U_{1-x}Th_xPt$ system that the substitution of Th in UPt stabilizes its orthorhombic phase. The variation of lattice parameters and unit cell volume across the series is depicted in figure 1.

Magnetization measurements have been performed on solid pieces of polycrystalline material for temperatures up to 40 K and magnetic fields up to 50 kOe, and magnetic susceptibility measurements between 1.7 and 300 K, both by means of a Quantum Design SQUID magnetometer. The specific heat was measured between 2.5 and 65 K using a standard adiabatic method. The electrical resistivity and magnetoresistance up to 80 kOe for samples with $x \geqslant 0.1$ were measured on bar-shaped samples between 4.2 K and 300 K by the standard dc four-point method and with the magnetic field applied perpendicular to the sample current direction. In some cases these measurements were extended down to 1.4 K. The electrical contacts were made using indium. For UPt, such quantities were measured using a low-frequency four-probe ac technique at temperatures from 1.8 to 300 K and in magnetic fields up to 140 kOe. Electrical contacts in this case were made with silver paint.

3. Results

3.1. Magnetization and susceptibility

The behaviour of the field dependence of the magnetization for our L-phase UPt (not shown here) is qualitatively similar to literature results for those of the L or H phases or mixtures of these (see for example [3], [5], [6], [17]), i.e. there is a large high-field susceptibility and the M–H hysteresis curves are extremely narrow. Extrapolation of M to $H = 0$ leads to a spontaneous moment at 1.7 K of 0.55 μ_B for UPt. This value is close to those reported in the literature for various phases of UPt. Magnetization isotherms for $U_{0.8}Th_{0.2}Pt$ and $U_{0.4}Th_{0.6}Pt$ are given in figures 2(a) and 2(b), respectively. As an example, the results in the former figure are representative of the behaviour of alloys for $x \leqslant 0.4$, which show ferromagnetic characteristics, while those in the latter figure are characteristic for alloys with $x \geqslant 0.5$, which are no longer magnetically ordered. Noteworthy for all the ferromagnetic

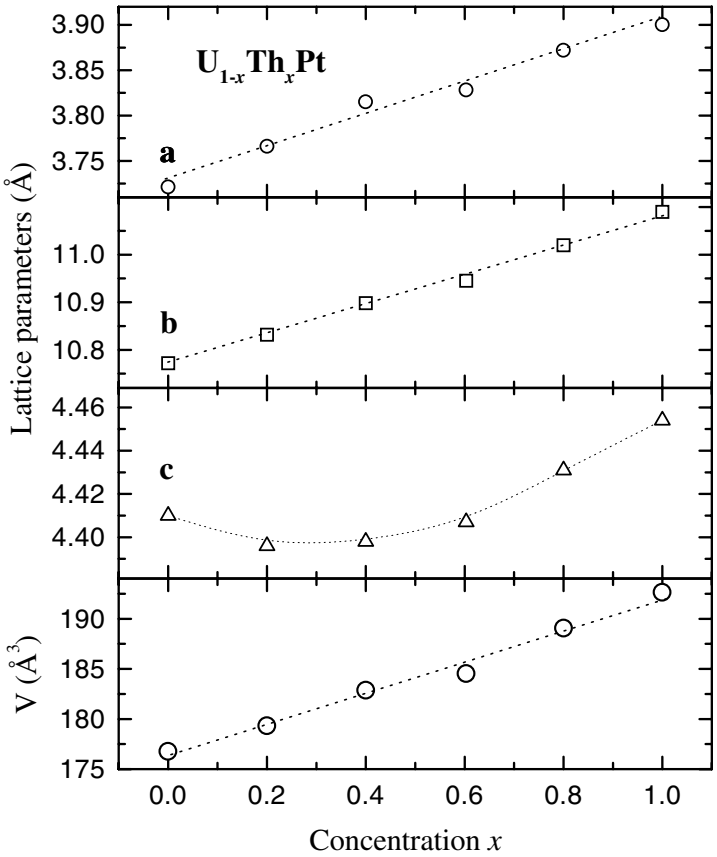

Figure 1. The variation of the room-temperature lattice parameter values and unit cell volume with Th concentration x for $U_{1-x}Th_xPt$ alloys. Note that Vegard's relationship is followed as indicated with dashed lines, except for the case of the c lattice parameter.

alloys is the relatively small hysteresis observed between the results obtained in increasing and subsequent decreasing magnetic fields, including those for the lowest-temperature isotherm. Also, all of the ferromagnetically ordered alloys ($x \leqslant 0.4$) display a clear lack of saturation in their magnetization curves at low temperatures. As mentioned above, such a large high-field susceptibility, χ_{hf}, has also been seen in previous studies on UPt: not only in magnetic fields up to 50 kOe [1, 5, 6], but even up to 350 kOe [3] the magnetization has not saturated.

In figures 3(a) and 3(b) the temperature dependences of the magnetization M and its temperature derivative dM/dT are respectively given. These results refer to measurements made in 5 kOe on samples initially cooled in zero field to a base temperature of 1.7 K. For $x = 0$ and 0.1 in addition to negative broad peaks at T_C, we also note the presence of small peaks in the $dM(T)/dT$ curves at lower temperature (see the inset of figure 3(b)). As we will discuss below, some anomalies in this temperature range have been observed also in other measurements. The Curie temperatures for the magnetically ordered alloys were first established from the Arrott plots of M^2 against H/M. Two representative sets of curves are given in figure 4(a) (for $x = 0.1$) and 4(b) (for $x = 0.5$). From the latter figure we see that even at the lowest temperatures, the extrapolation of high-field H/M data does not cross the M^2 axis, indicating the absence of spontaneous magnetization. As mentioned above, we have

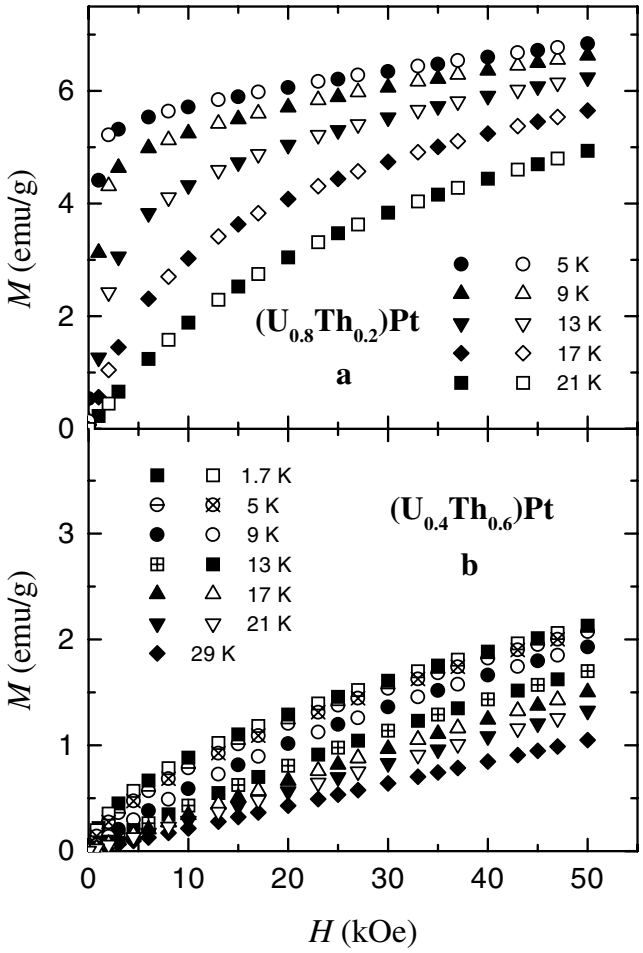

Figure 2. Magnetization isotherms for (a) $U_{0.8}Th_{0.2}Pt$ and (b) $U_{0.4}Th_{0.6}Pt$, representing the magnetically ordered and magnetically non-ordered alloys respectively. The closed symbols were measured during increasing field scans and open symbols during subsequent decreasing field scans.

also determined values of T_C from the observed minima in the dM/dT–T curves. Values of T_C as obtained from the various physical properties measured in this investigation, including the specific heat (see discussion below), are given in table 1.

In figure 5 the temperature dependence of the inverse susceptibility $\chi^{-1}(T)$ as measured in 5 kOe is given. The solid lines are obtained by least-squares (LSQ) fitting of the data against a modified Curie–Weiss relation

$$\chi^{-1}(T) = \left[\chi_0 + \frac{N_A \mu_{eff}^2}{3k_B(T - \Theta_p)}\right]^{-1} \tag{1}$$

where k_B is Boltzmann's constant, N_A is Avogadro's number and χ_0 is a temperature-independent term. Values of χ_0, μ_{eff} and Θ_p are given in table 1 for the different alloys. In the case of L-phase UPt, these values, amounting to 1.13×10^{-5} emu/mol U, 1.97 μ_B and 14.3 K respectively, are comparable to those reported by Prokeš *et al* [6]. We have also found that our data of the reciprocal susceptibility fit well to the data extending up to 1000 K, which

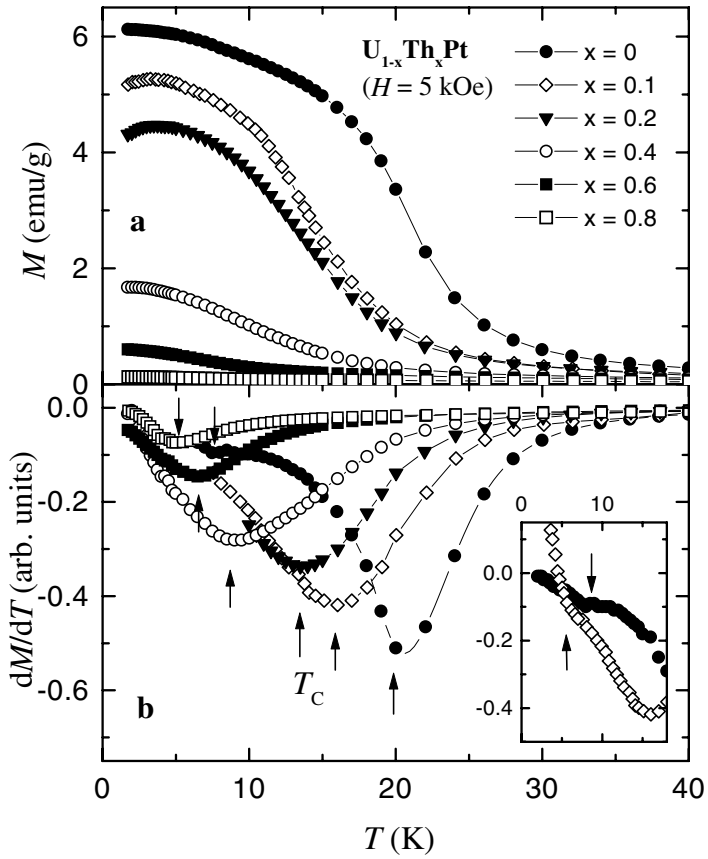

Figure 3. The temperature dependence of (a) the magnetization M, and (b) the derivative $\mathrm{d}M/\mathrm{d}T$ for various $U_{1-x}Th_xPt$ alloys. The arrows mark the respective Curie temperatures. The inset shows the low-temperature data for $x = 0$ and 0.1 on expanded scales.

Table 1. The values of the Curie temperature T_C for alloys in the system $U_{1-x}Th_xPt$ as determined from Arrott plots (I), minima in $\mathrm{d}M/\mathrm{d}T$ (II) and specific heat (III). Values of χ_0, μ_{eff} and Θ_p as obtained from fits of the inverse susceptibility $\chi^{-1}(T)$ according to (1) are also given.

	T_C [±0.5 K]			$\chi_0 \times 10^3$	μ_{eff}	Θ_p
x	I	II	III	[±0.2 emu/mol U]	[±0.2 μ_B]	[±0.5 K]
0	19.0	20.5	19.0	1.13	1.97	14.3
0.1	17.0	16	16.0	0.3	2.51	15.5
0.2	15.5	14	15.1	0.4	2.71	16.5
0.4	9.0	9.1	[a]	0.8	2.78	8.8
0.5	—	(6.6)	—	0.8	2.76	−2.2
0.6	—	(6)	—	0.8	2.66	−12.3
0.7	—	(4.7)	—	0.8	2.73	−16.3
0.8	—	(4.5)	—	0.8	2.81	−16.5

[a] The transition is reminiscent of that in spin-glass-like materials.

were earlier reported by Frings *et al* [3]. A distinct curvature was observed by these authors almost up to 1000 K and this indicates the presence of large magnetocrystalline anisotropy

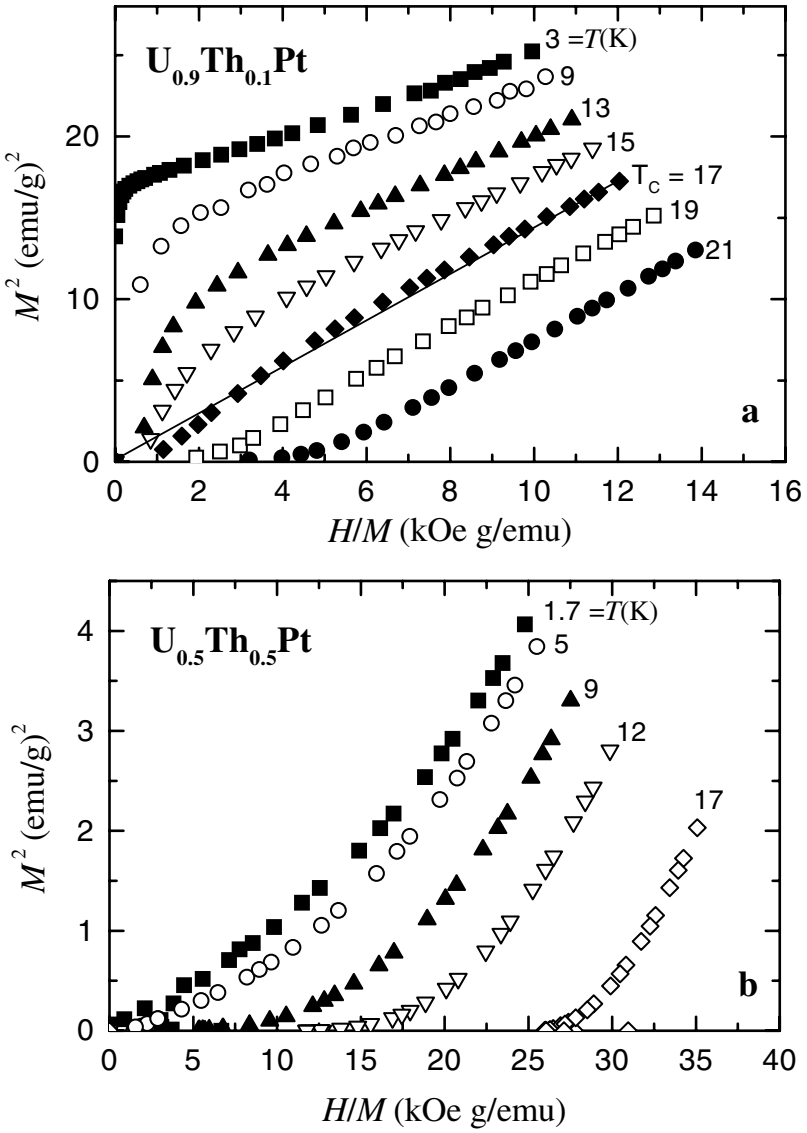

Figure 4. Arrott plots for (a) $U_{0.9}Th_{0.1}Pt$ and (b) $U_{0.5}Th_{0.5}Pt$ representing the magnetically ordered and magnetically non-ordered alloys respectively.

in UPt, as has recently been confirmed by UPt single-crystal measurements [17] up to room temperature. It is likely that this type of anisotropy has its origin in the crystal-electric field interactions in this intermetallic compound. Consequently, the 5f electrons of uranium atoms in this compound should be treated as localized with only some small degree of hybridization with the conduction electrons, rather than itinerant, as has recently been suggested by Prokeš *et al* [6, 17]. Also photoemission and bremsstrahlung isochromat spectra point to higher 5f electron localization in UPt, for which the completely filled Pt5d band states make the f–d hybridization negligible [21]. For a polycrystalline sample of an anisotropic magnetic material one should be careful to attach particular physical significance to any of the values obtained

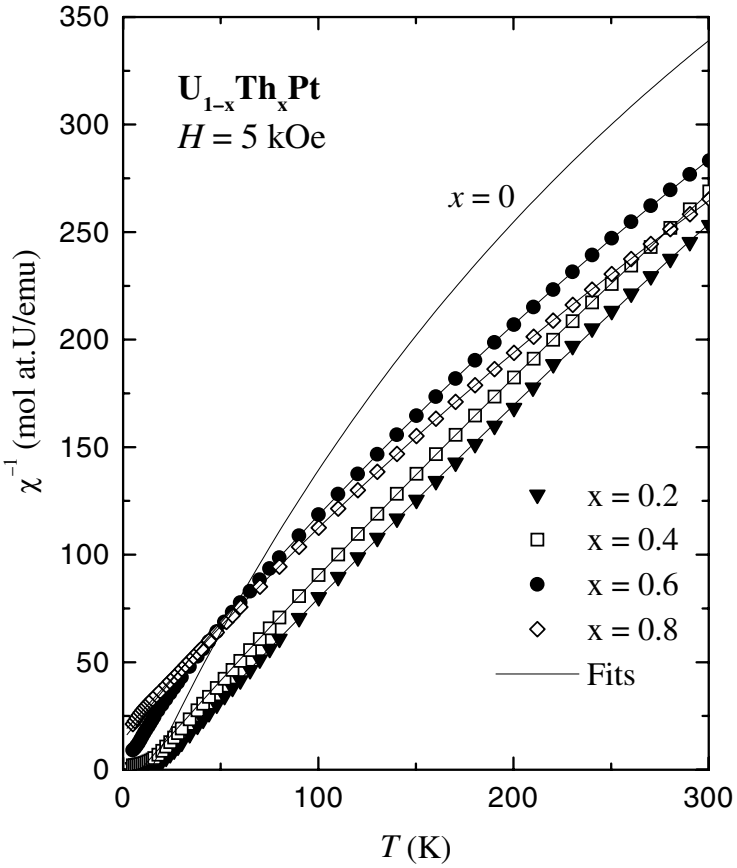

Figure 5. The temperature dependence of the inverse magnetic susceptibility χ^{-1} for various $U_{1-x}Th_xPt$ alloys. The solid lines are least-squares fits to a modified Curie–Weiss law (1) and the values of fit parameters are given in table 1. For the purpose of clarity, the experimental points for UPt are not shown here.

Table 2. Values of γ_{5f}, Δ and g as obtained from fits of the specific heat $C_{5f}(T)$ according to (3), and values ρ_0, b and A from the fits of the resistivity $\rho_{5f}(T)$, according to (4), are given.

x	γ_{5f} [J K^{-2} mol^{-1}/at U]	Δ [K]	g [K$^{-1/2}$]	ρ_0 [$\mu\Omega$ cm]	b [K^{-1}]	A [$\mu\Omega$ cm K^{-2}]
0	0.122(2)	19 (1)	3.3(1)[a]	41(2)	0.46(5)	0.284 (1)
	0.151(3)	35(2)	2.9(5)[b]			
0.1	0.142 (1)	13 (1)	0.96(5)	90(2)	0.88(5)	0.011(2)
0.2	0.149(1)	11 (1)	1.14(9)	95(2)	0.87(5)	0.010(2)
0.4	0.155(2)	10 (2)	1.07(2)	64(2)	0.04(5)	0.086(2)
0.6	0.175(2)	—	—	51(2)	—	0.060(3)
0.7	0.141(2)	—	—	29(2)	—	0.038(1)
0.8	0.135(5)	—	—	24(2)	—	0.033(2)

Fitting to (3) [a] below 10 K and [b] above this temperature.

for the parameters χ_0, $\mu_{\rm eff}$ and $\Theta_{\rm p}$. Nevertheless, as seen in table 1, $\mu_{\rm eff}$ and χ_0 approach almost constant values of respectively about 2.75 ± 0.05 $\mu_{\rm B}$/U and 0.8×10^{-3} emu/mol U already for the $x \geqslant 0.2$ alloys.

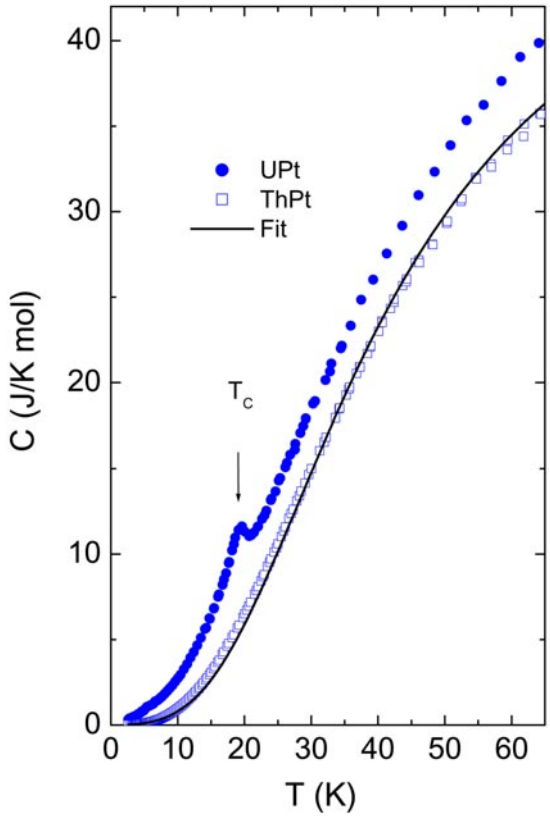

Figure 6. The temperature dependence of the specific heat C of UPt and ThPt. The solid line is a fit of the ThPt data to (2).

3.2. Specific heat

The specific heat C was determined between 2.5 K and 65 K for alloys of the series with $x = 0$, 0.1, 0.2, 0.4, 0.6, 0.7, 0.8 and 1.0. As an example of our results we plot in figure 6 $C(T)$ for UPt and for the non-magnetic homologue ThPt. The solid line in the figure indicates an LSQ fit of the ThPt data to

$$C(T) = 9R(T/\Theta_D)^3 \int_0^{\Theta/T} \frac{x^4 e^x \, dx}{(e^x - 1)^2} + \gamma_{ThPt} T \tag{2}$$

with $x = \eta\omega/k_B$. The first term is the Debye description of the phonon contribution to $C(T)$ and a value of $\Theta_D = 170$ K is obtained from the data in figure 6. The second term gives the small electronic contribution to the specific heat with $\gamma_{ThPt} = 2.2$ mJ mol^{-1} K^{-2}. Generally our data for $C(T)$ of ThPt are in agreement with the previous data of Luengo *et al* [2]. However, the Θ_D value of the above non-magnetic reference taken here for that of UPt is lower than 190 K as used in [6] in an approximation of the phonon contribution. This difference of course will influence the derived values of $C_{5f}(T)$. We ignored the expected small difference in Debye temperature between U and Th compounds because of the small mass difference of about 1.3% between these compounds.

In figure 7 we show a sum of the electronic and magnetic contributions to the specific heat as C_{5f}, obtained by subtracting the specific heat of ThPt as parametrized above using (2)

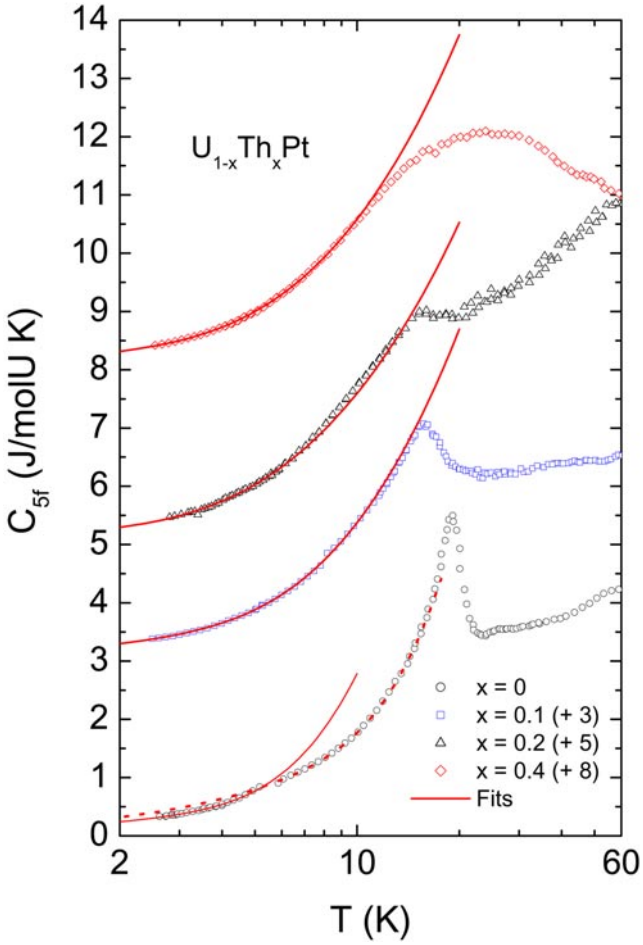

Figure 7. The temperature dependence of the magnetic and electronic contribution (C_{5f}) to the specific heat of $U_{1-x}Th_xPt$, where $x = 0$, 0.1, 0.2 and 0.4 as obtained by subtracting the specific heat of ThPt as a phonon contribution. The solid lines are least-squares fits to (3) with the fit parameters given in table 2. Note the offset of curves for $x \geqslant 0.1$ as indicated in the legend of the figure.

from the measured data for alloys with $x = 0$, 0.1, 0.2 and 0.4. As seen from this figure, the data for UPt show a clear λ-shaped anomaly at $T_C = 19.0(5)$ K, while for the remaining alloys this anomaly becomes more and more broadened with increasing x. This is especially true for $x = 0.4$, where a very wide anomaly in $C_{5f}(T)$, centred at about 22 K, is observed, which is rather reminiscent of that encountered in spin-glass-like materials. With Th substitution the magnitude of the anomaly at T_C is rapidly reduced and in the case of the $x = 0.4$ alloy, for which the transition to the ordered state occurs at T_C of about 10 K (see table 1), this transition is practically unseen in the $C_{5f}(T)$ curve. Furthermore, the data in the magnetic ordered region in figure 7 are LSQ fitted (solid lines) to the equation

$$C_{5f} = gT^{1/2}\exp(-\Delta/T) + \gamma_{5f}T. \tag{3}$$

The first term is an expression for the magnon specific heat and has been given by Andersen and Smith [22]. Here Δ is an energy gap in the magnon spectrum and an expression for

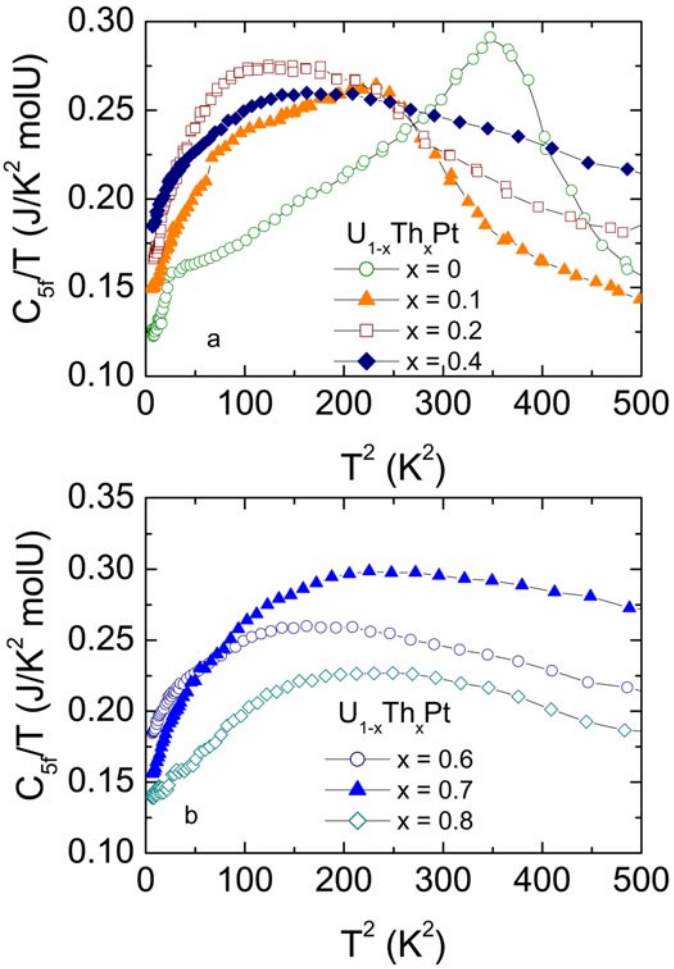

Figure 8. The temperature dependences of C_{5f}/T against T^2 for various $U_{1-x}Th_xPt$ alloys: (a) $x = 0$, 0.1, 0.2 and 0.4 and (b) $x = 0.6$, 0.7 and 0.8.

the parameter g is given in [22]. The 5f-electron contribution to the specific heat, $\gamma_{5f}T$, is considerably enhanced with respect to that of the non-magnetic ThPt homologue. Values of Δ, g and γ_{5f} obtained by LSQ fitting the $C_{5f}(T)$ data for the various magnetically ordered compounds are given in table 2. It turns out that such a fitting made for the UPt data has to be made in two separate temperature ranges, i.e. up to about 10 K and above this temperature. These fits for UPt are indicated in figure 7 by solid and dashed lines respectively. The necessity of separating the UPt C_p-data into two regions is well evident from figure 8(a), where the C_{5f}/T–T^2 curves are presented for the four compositions given above. It is clear that for UPt a distinct break in this curve occurs at about 10 K. It is noted that an extrapolation of C_{5f}/T to $T = 0$ K yields similar values to those determined from (2). In figure 8(b) such curves are shown for the magnetically non-ordered alloys with $x = 0.6$, 0.7 and 0.8. The results of extrapolation to $T = 0$ K for these alloys are also given in table 2. It is clear that the values of C_{5f}/T, for all the concentrations studied by us, are considerably enhanced at low temperatures (see figure 8 and table 2). The $\gamma_{5f}(0)$ values found for the samples that are not magnetically

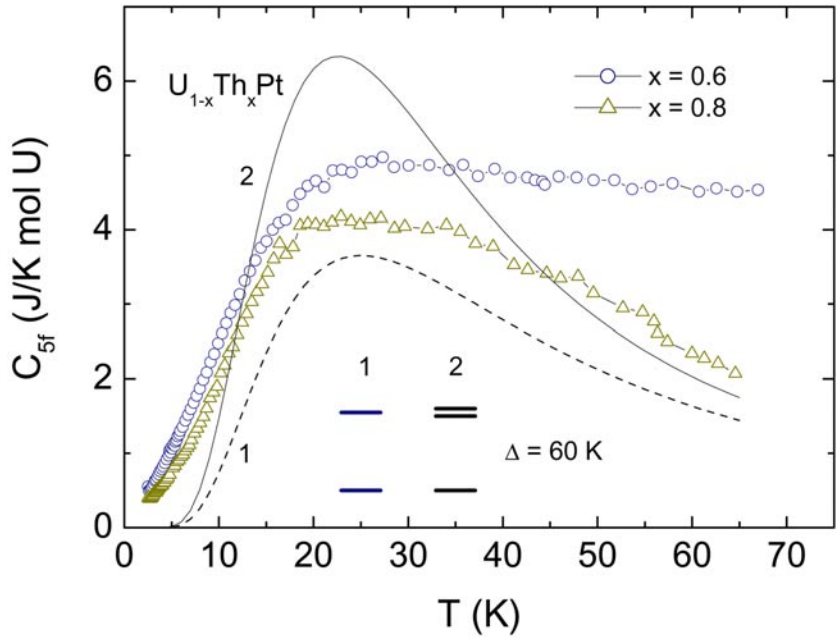

Figure 9. The C_{5f} subtracted data for $x = 0.6$ (open circles) and 0.8 (open triangles). For sake of illustration dashed and solid lines which represent calculated Schottky anomalies for crystal field schemes shown in the figure are indicated (see the text).

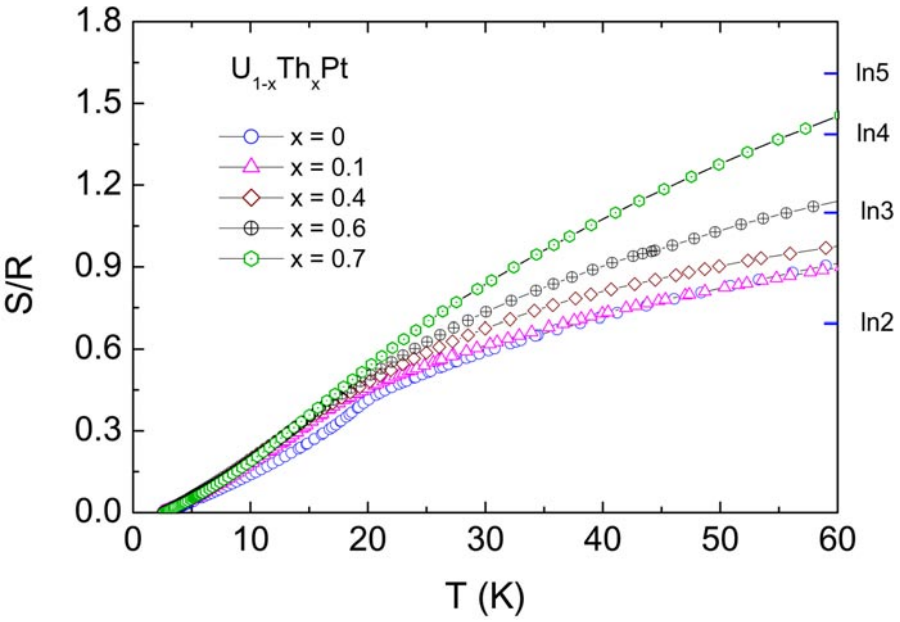

Figure 10. The temperature dependence of the total entropy S of $U_{1-x}Th_xPt$, where $x = 0$, 0.1, 0.4, 0.6 and 0.7.

ordered (see table 2) are large and comparable to those for samples pertaining to the ordered region.

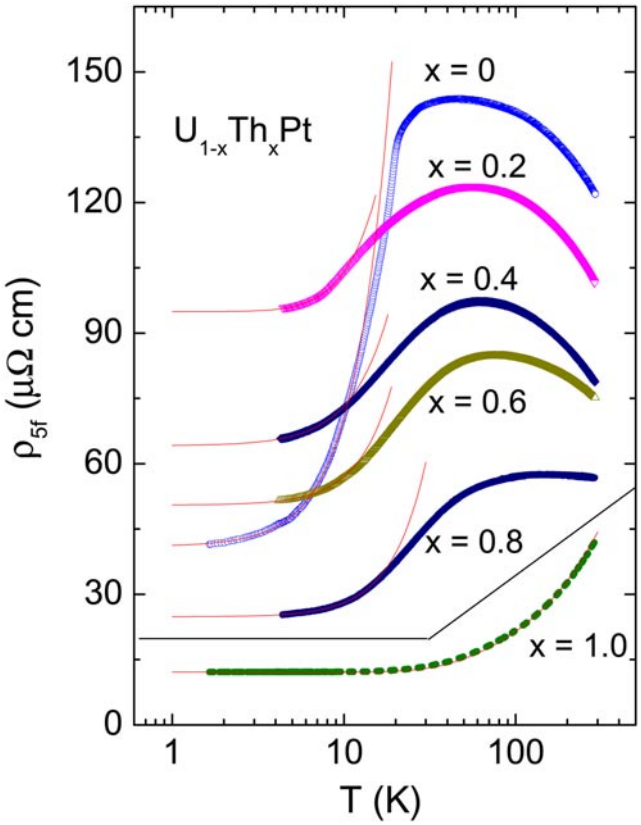

Figure 11. The temperature dependences of the 5f derived resistivity, ρ_{5f}, of $U_{1-x}Th_xPt$ alloys ($0 \leqslant x \leqslant 0.8$) and fits of this quantity against (4). The ρ_{5f} values are obtained by subtracting the phonon temperature dependent part of the resistivity of ThPt from the measured values of these uranium-containing alloys. Measurements of the latter ($x = 1.0$) are also given in the figure and the solid line in this case is a Bloch–Grüneisen fit.

The $\gamma(0)$ values given in table 2 indicate the medium heavy-fermion character of these samples and these values are not much changed by the dilution process. As is also apparent from table 2 our value of $\gamma(0)(= 122$ mJ K^{-2} mol^{-1}) for UPt is somewhat higher than those previously reported, namely 80 [8], 105 [6] and 115 mJ (K^{-2} U mol)$^{-1}$ [6]. Previously, only Prokeš *et al* [6] fitted their low-temperature heat capacity data to the magnon expression containing a gap Δ. They found $\Delta = 20.1(2)$ K, which can be compared with our low-temperature value of $\Delta = 19(1)$ K (see table 2). On the other hand, our high-temperature value of 35(3) K (table 2) is closer to that of 40 K derived in [17] for H-phase UPt using single-crystal magnetization data at low temperatures.

As an example, we illustrate in figure 9 the qualitative similarity observed between the extracted C_{5f}–T curve for $x = 0.6$ and 0.8 and that calculated for two level schemes of crystal-field splitting (Schottky anomaly) with the ratio of the degeneracy $g_R = 1$ and 2 between the ground and excited levels (see the caption of figure 9). One should bear in mind that there exists in $C_{5f}(T)$, apart from a Schottky contribution, also the contribution due to the electronic heat capacity which at high temperatures remains rather undetermined. We furthermore refrain from discussing the valence of the U atom in the UPt–ThPt pseudo-binary system and other details of crystal-field splitting in view of the present state of research results on this system.

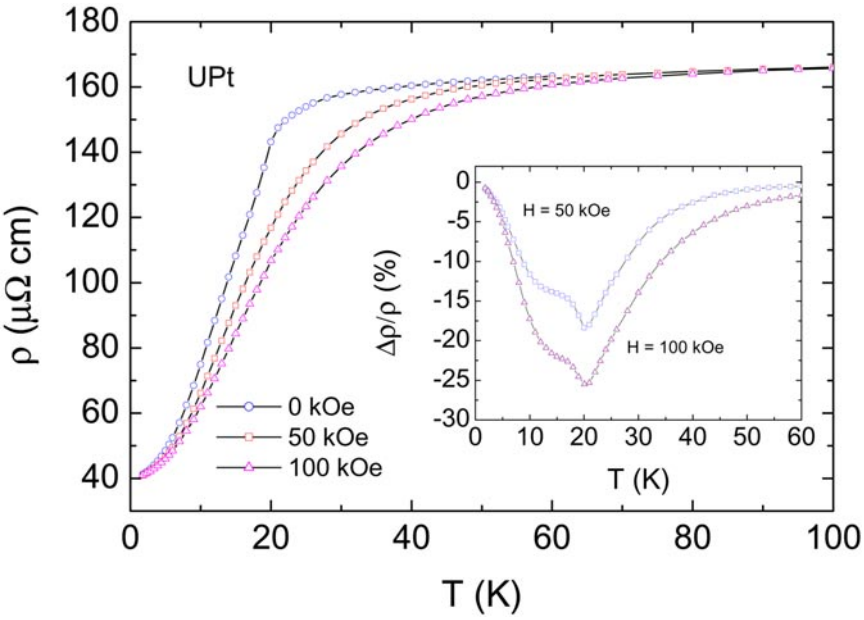

Figure 12. The electrical resistivity as function of temperature for UPt in 0, 50 and 100 kOe. The inset shows the magnetoresistance $\Delta\rho(T)/\rho_0$ measured at 50 and 100 kOe as a function of temperature.

The total entropy $S(T)$ for the $U_{1-x}Th_xPt$ alloys has been calculated by integrating C_{5f}/T against T up to 65 K, the maximum temperature for which specific heat data were taken. These results are depicted in figure 10. For all the magnetically ordered alloys the entropy increases fairly rapidly with increasing temperature to reach a value of approximately $R\ln 2$ at their respective Curie temperatures. However, $S(T)$ has the tendency to increase further with increasing temperature in the paramagnetic region, which is in general agreement with previous studies in the case of UPt [2, 6]. This suggests a doublet as a magnetic ground state for this alloy. For higher Th contents as for $x = 0.6$ and 0.7, the $S(T)$ function reaches at $T = 65$ K values that are even larger than $S = R\ln 4$. This may point to a decrease of the overall crystal field splitting energy with increasing x and hence the populating of higher crystal-field levels at higher temperatures when diluting UPt through Th substitution. However, one should caution that several uncertainties enter these calculations, e.g. the appropriate value of Debye temperature to be used, not taking the electronic heat capacity contribution into account and the large error in subtracting the phonon part from the total heat capacity in the case of the most dilute compositions and subsequent conversion into entropy per uranium ion.

3.3. Resistivity and magnetoresistance

The magnetic part of the resistivity ρ_{5f} for various $U_{1-x}Th_xPt$ alloys is plotted in figure 11. We obtained ρ_{5f} by subtracting the phonon contribution, which was based on fitting the temperature dependence of ThPt resistivity (also shown in figure 11) against a Bloch–Grüneisen function, from the measured data for these alloys. The results for the magnetically ordered alloys ($x = 0$, 0.2, 0.4) were fitted at low temperatures according to an expression containing the magnon

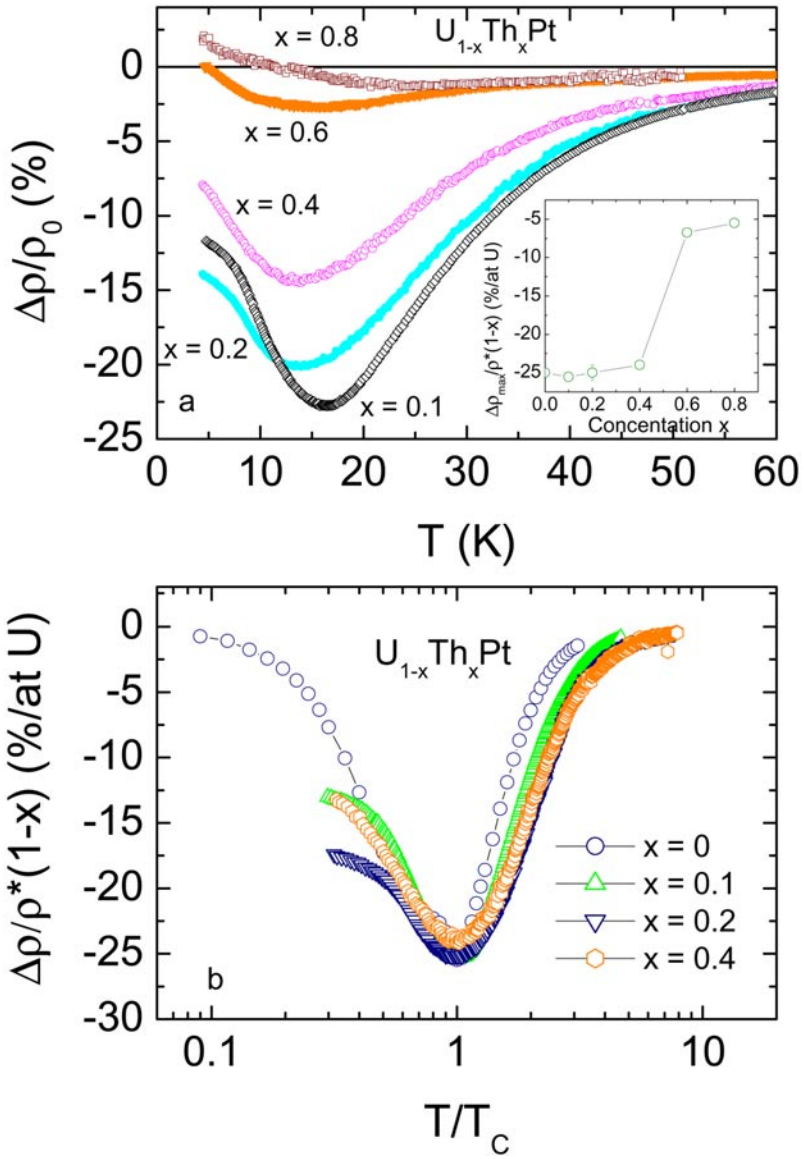

Figure 13. (a) The temperature dependences of the magnetoresistance $\Delta\rho(T)/\rho_0$ measured at 80 kOe for $U_{1-x}Th_xPt$ alloys for various x-values indicated in the figure. The inset shows the concentration dependence of the maximum value $\Delta\rho_{max}/\rho$ normalized per U atom. (b) The normalized magnetoresistance per U atom, measured at 100 kOe for UPt and at 80 kOe for $U_{1-x}Th_xPt$ alloys with x up to 0.4 as function of T/T_C.

energy-gap Δ [22]

$$\rho_{5f} = \rho_0 + bT\left(1 + \frac{2T}{\Delta}\right)\exp(-\Delta/T) + AT^2. \tag{4}$$

In (4), ρ_0 is a temperature-independent term that gives the defect scattering, an expression for b is given in [22] and as the last term in (4) we include a Fermi-liquid-like contribution to the electron scattering. In the LSQ fitting procedure Δ was fixed at the values obtained in fitting

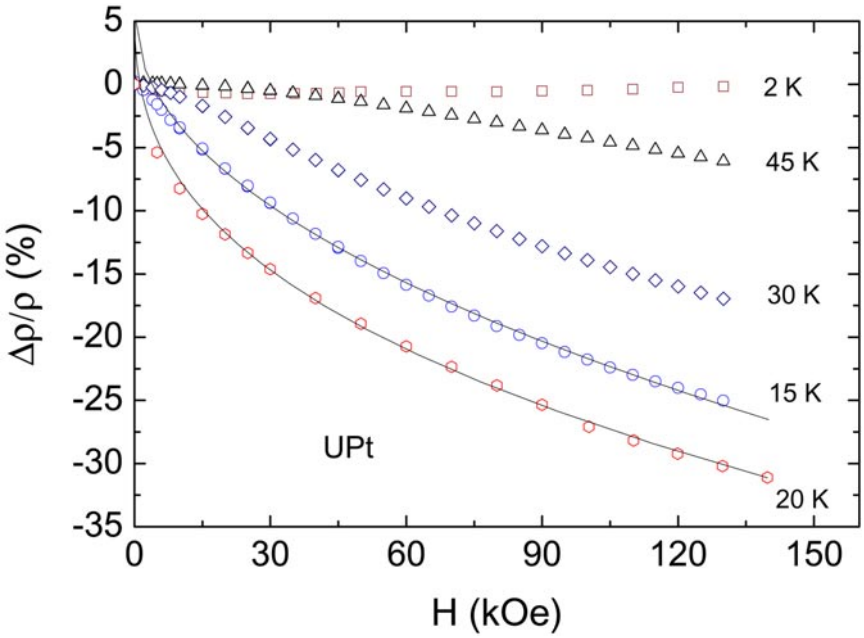

Figure 14. The magnetoresistance $\Delta\rho(H)/\rho_0$ of UPt as a function of applied magnetic field up to 140 kOe at various temperatures.

the specific heat data (see table 2). The fits for ρ_{5f} are indicated in figure 11 as weak solid lines and the parameters ρ_0, b and A for the various alloys are given in table 2. For the alloys that are non-magnetically ordered ($x = 0.6$, 0.7 and 0.8) we omit the spin-wave term from (4) and LSQ fit our data against $\rho_{5f} = \rho_0 + AT^2$.

At temperatures above 100 K, negative temperature coefficients of the resistivity ρ_{5f} are observed for all the alloys with $x \leqslant 0.6$, indicating incoherent Kondo scattering of electrons. For higher Th concentrations, such a tendency is likely expected above room temperature.

Finally, we present in figure 12 the electrical resistivity of UPt as a function of temperature at 0, 50 and 100 kOe. A large influence of magnetic field on the resistivity is seen in this figure. In the inset of this figure the $\Delta\rho/\rho$–T dependences at 50 and 100 kOe are demonstrated. These data illustrate the pronounced effect of an applied magnetic field on ρ in the vicinity of T_C. The $\Delta\rho(T)/\rho_0$ curves for UPt display a well defined negative minimum at $T_C = 19$ K and a shoulder near 12 K. These two anomalies in $\Delta\rho(T)/\rho_0$ have also been previously observed by Petrenko *et al* [12]. The mechanism responsible for this low-temperature shoulder is thought to be connected with that leading to an anomaly in the dM/dT–T curves near this temperature (see the inset of figure 3(b)), as well as to a small anomaly at a temperature slightly below about 10 K, reported by Kamma *et al* [4] in their thermal expansion and ac-susceptibility investigations on the pure L-phase UPt. In contrast to UPt, the other alloys investigated up to 80 kOe (figure 13(a)) show only one, though more broadened, negative minimum. For the $x = 0.1$ alloy the MR reaches near T_C a value as large as -23%, which is not expected for a normal ferromagnet. It is useful to investigate the concentration dependence of the maximum MR per U atom, $\Delta\rho_{max}/\rho$ (at U). The data shown in the inset of figure 13(a) indicate that replacing uranium in UPt by thorium does not change $\Delta\rho_{max}/\rho$ (at U) at least for x up to

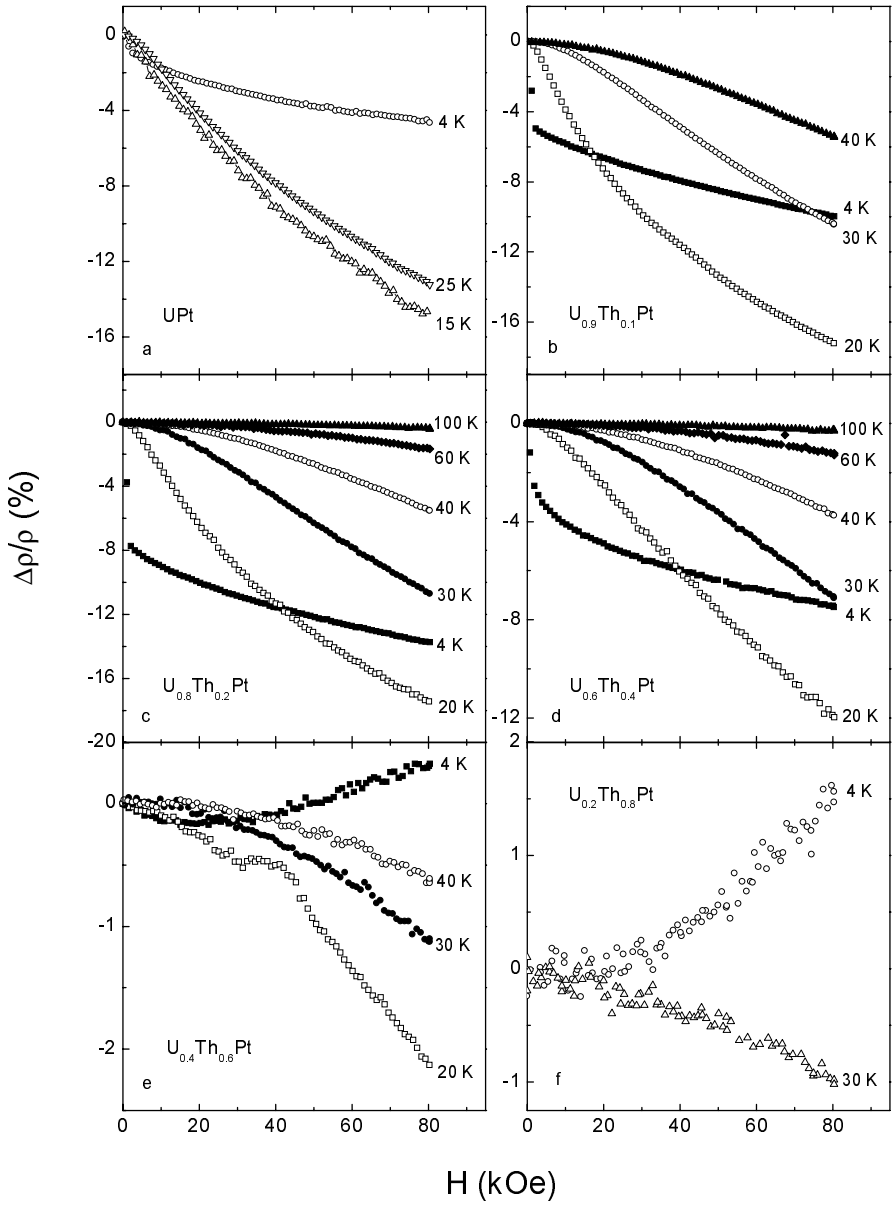

Figure 15. Magnetoresistance isotherms $\Delta\rho(H)/\rho_0$ for various $U_{1-x}Th_xPt$ alloys, *viz.* (a) UPt, (b) $U_{0.9}Th_{0.1}Pt$, (c) $U_{0.8}Th_{0.2}Pt$, (d) $U_{0.6}Th_{0.4}Pt$, (e) $U_{0.4}Th_{0.6}Pt$ and (f) $U_{0.2}Th_{0.8}Pt$.

0.4. The reduction in $\Delta\rho_{max}/\rho$ (at U), however, takes place just for $x = 0.6$ and 0.8, where no long-range order down to 1.7 K could be resolved. To get further information about the MR behaviour of the $U_{1-x}Th_xPt$ system, we have also used the scaling of $\Delta\rho/\rho$ (at U) as a function of T/T_C (figure 13(b)). As can be seen, the data fall rather well onto a common curve, implying that in the ordered region the substitution effect appears mainly through the volume effect.

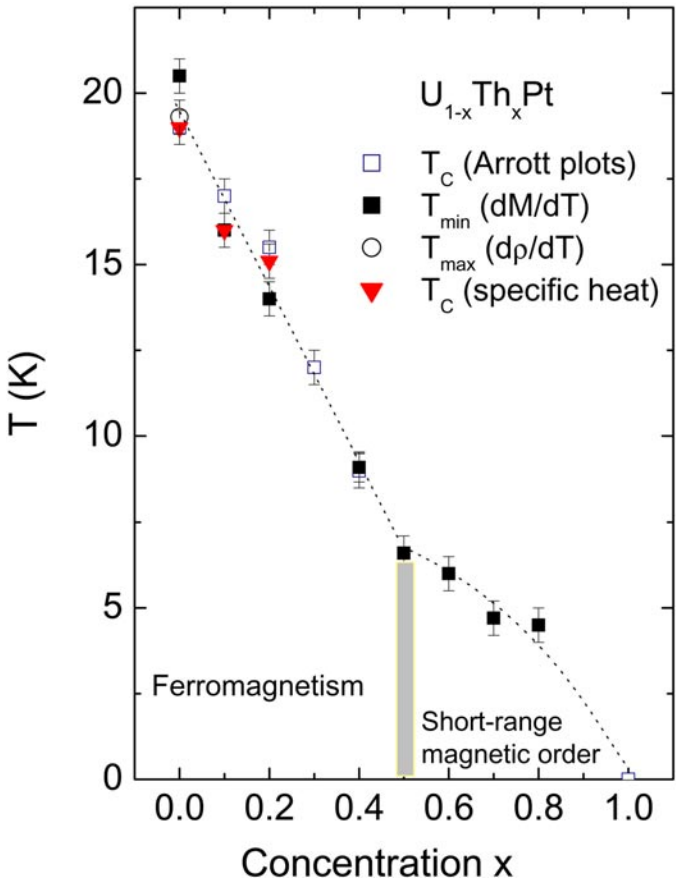

Figure 16. Tentative magnetic phase diagram of the UPt–ThPt system (L phase).

The $\Delta\rho(H)/\rho_0$ isotherms measured in fields up to 140 kOe and various temperatures up to 45 K for UPt are presented in figure 14. Those for isotherms in the critical region, i.e. at 15 and 20 K, can be described by a power-law dependence H^n, where $n = 0.37$ for the 20 K curve and 0.48 for the 15 K curve. Even in 140 kOe these curves are still far from saturation despite the fact that the $\Delta\rho(H)/\rho_0$-value in 140 kOe at 20 K is as high as -32%. This value can be compared with those found recently for the ferromagnets URhSi (-40%) and URhGe (-36%) [23]. It has been proposed that the large values of the MR observed in the latter compounds are associated with the magnetic polaron effect.

The magnetoresistance for UPt and the remaining alloys in magnetic fields up to 80 kOe are displayed in figures 15(a)–15(f). The MR is large and predominantly negative with the exception of the 4 K isotherms for alloys with $x = 0.6$ and 0.8, which show positive MR. It is likely that positive MR in the latter case is due to a significant contribution of the normal magnetoresistance associated with potential scattering, which plays a dominant role at low temperatures and at high magnetic fields for these dilute concentrations. We note that the data were taken on polycrystalline samples and therefore preclude any conclusions pertaining to the details of the magnetic ordering. At higher temperatures for all U-containing alloys in the series, one may attach the systematic negative MR to the suppression of Kondo type, spin-flip scattering. At lower temperatures on the other hand, the removal of spin disorder by

the applied magnetic field, as is the case for magnetically ordered samples, seems to become dominant over the contribution due to the Kondo effect. Hence, the $\Delta\rho(H)/\rho_0$ isotherms are seen to concur with the behaviour observed in $\Delta\rho(T)/\rho_0$, with the most significant effect of the magnetic field near T_C. At $T = 4$ K for the $0.1 \leqslant x \leqslant 0.4$ alloys we observe in small fields, with $H \leqslant 5$ kOe, a sharp decrease in ρ as evidenced by a drop in $\Delta\rho(H)/\rho_0$ (see figures 15(b)–15(d)), and we associate this with the effect that the external field has on the spin system in the ordered region. Surprisingly, this effect is not seen so distinctly for undiluted UPt.

Finally, in figure 16 we present a tentative magnetic phase diagram of the UPt–ThPt system based on results of various measurements.

4. Conclusion

Magnetic, electronic and thermodynamic properties are reported on UPt (L phase, $T_C = 19$ K) and $U_{1-x}Th_xPt$ alloys that crystallize in the orthorhombic CrB-type unit cell. In the case of the former compound, this is in contrast with some earlier work on UPt for which the samples apparently contained both the orthorhombic and monoclinic phases. On the other hand, the latest studies by Prokeš *et al* [6, 17] have shown that their samples exhibited predominantly the monoclinic structure with T_C near 27 K. In our study the $U_{1-x}Th_xPt$ alloys with $0 \leqslant x \leqslant 0.4$ have been found to be ferromagnetic. On the basis of Arrott plots, we have shown that alloys with $x \geqslant 0.5$ are no longer spontaneously ordered, although the magnetization curves reveal signatures of ferromagnetic character. We also note that the minima in the dM/dT–T curves used to determine T_C have also been observed for alloys with $x \geqslant 0.5$. We have associated them with the appearance of short-range ferromagnetic order for compositions in this range of concentration.

To describe the electronic and magnetic contributions to the specific heat C_{5f} and electrical resistivity ρ_{5f} we used in the magnetically ordered region expressions that include both the magnon energy-gap Δ and the γ_{5f} and AT^2 terms respectively. Surprisingly, the moderately enhanced values of γ_{5f} turned out to be close to each other for both the magnetically ordered and non-ordered alloys; this parameter was practically only slightly dependent on the U content across the series of alloys and hence we associate this with the strongly correlated 5f-electron behaviour of Kondo type.

For U-rich samples, the persistence of a large negative MR in the paramagnetic region suggests the presence of the Kondo-like interaction, which is also supported by a negative temperature coefficient of the resistivity observed for these alloys at higher temperatures.

A comparison of our results with those reported for the $U_{1-x}La_xPt$ system [11] shows agreement in characteristics such as the composition range of magnetic order, the large reduction in spin-disorder resistivity upon dilution by a non-magnetic element and a negative temperature coefficient of the 5f-electron resistivity observed for some U-rich alloys in both systems, which suggests the presence of the Kondo mechanism in the electron scattering.

It is evident from the above that the $U_{1-x}Th_xPt$ alloys present an interesting 5f-electron system for studying the competing magnetic, Kondo and crystal-electric field interactions.

Acknowledgments

We thank Mr R Gorzelniak and Mr D Badurski for their technical assistance in this work. Financial support from the South African National Research Foundation under both its Open Research Program and its International Science Liaison Program, the University of the Witwatersrand Research Committee and the State Committee for Scientific Research (KBN) in Poland within grant no 2P03B 150 17 are gratefully acknowledged.

References

[1] Huber J G, Maple M B and Wohlleben D 1975 *J. Magn. Magn. Mater.* **1** 58
[2] Luengo C A, Maple M B and Huber J G 1976 *J. Magn. Magn. Mater.* **3** 305
[3] Frings P H, Franse J J M, de Boer F R and Menovsky A 1983 *J. Magn. Magn. Mater.* **31–34** 240
[4] Kamma C F, Frings P H, Klaasse J C P and Franse J J M 1983 *Physica* B **119** 72
[5] Frings P H and Franse J J M 1985 *J. Magn. Magn. Mater.* **51** 141
[6] Prokeš K, Klaasse J C P, Hagmusa I H, Menovsky A A, Brück E H, de Boer F R and Fujita T 1998 *J. Phys.: Condens. Matter* **10** 10 643
[7] Franse J J M, Frings P H, de Boer F R and Menovsky A 1981 *Physics of Solids under High Pressure* ed J S Schilling and R N Shelton (Amsterdam: North-Holland) p 181
[8] de Podesta M, Lester C, McEwen K A, Espeso J and Gómez Sal J C 1995 *J. Magn. Magn. Mater.* **140–144** 1359
[9] Lawson A C 1970 *Phys. Lett.* A **33** 231
[10] Hill H H and Elliott R O 1971 *Phys. Lett.* A **35** 75
[11] Rodríguez Fernández J, Argüelles M A, Espeso J I, Gómez Sal J C and McEwen K A 1997 *Physica* B **230–232** 86
[12] Petrenko O V, Andreev A V and Kovácik V 1994 *IEEE Trans. Magn.* **30** 1211
[13] Franse J J M, Frings P H, van der Liet A, Menovsky A and de Visser A 1983 *Physica* B **123** 72
[14] Lawson A C, Williams A, Huber J G and Roof R B 1986 *J. Less-Common Met.* **120** 113
[15] Franse J J M., Menovsky A A, de Visser A, Frings P H and Vettier C 1987 *J. Magn. Magn. Mater.* **70** 351
[16] Frings P H, Vettier C, Dommann A, Hulliger F and Menovsky A A 1989 *Physica* B **156/157** 832
[17] Prokeš K, Fujita T, Brück E H, de Boer F R and Menovsky A A 1999 *Phys. Rev.* B **60** R730
[18] Dwight A E 1969 *Developments in the Structural Chemistry of Alloy Phases* ed B C Giessen (New York: Plenum) p 181
[19] Dommann A and Hulliger F 1988 *Solid State Commun.* **65** 1093
[20] Gómez Sal J C, McEwen K A, Espeso J I, Ellerby M, Rodríguez Fernández J M, de Podesta M and Blanco J A 1994 *Physica* B **199/200** 514
[21] Laubschat C, Grentz W and Kaindl G 1988 *Phys. Rev.* B **37** 8082
[22] Andersen N H and Smith H 1979 *Phys. Rev.* B **19** 384
[23] Tran V H and Troć R 1998 *Phys. Rev.* B **57** 11 592